World Journal of Engineering Research and Technology
WJERT
www.wjert.org
SJIF Impact Factor: 5.924

FINITE ELEMENT ANALYSIS OF SMALL VERTICAL AXIS WIND TURBINES

Dong-Yang Wu[1]*, Jian-Fan[2], Xiu-Qin Chen[2], Jian-Yang Song[2] and Jiang-Bo Tong[2]

[1]Hangzhou Oxygen Plant Group Co., Ltd, Hangzhou 310002, China.
[2]College of Mechanical Engineering, Quzhou University, Quzhou, 324000, China.

Article Received on 20/01/2020 **Article Revised on 10/02/2020** **Article Accepted on 02/03/2020**

***Corresponding Author**
Dong-Yang Wu
Hangzhou Oxygen Plant Group Co., Ltd, Hangzhou 310002, China.

ABSTRACT

Vertical axis wind turbine is widely used in wind power generation because of its simple structure, high reliability and automatic windward. In order to study the influence of shaft material, blade material and wind speed on the wind wheel of a small vertical axis wind turbine, this paper makes a finite element analysis of the wind wheel of small vertical axis wind turbine through the orthogonal experimental method. The results show that the maximum displacement always appears in the upper part of the wind turbine blade, and the maximum stress always appears in the bottom surface of the wind wheel main shaft; when the wind speed is small, the displacement and stress of shaft material and blade material change little. Then based on the ANSYS Workbench software, the modal analysis of the wind wheel shows that the natural frequency of the wind wheel is 6.05 *Hz*, so the frequency added by the wind wheel should avoid 6.05 *Hz* to prevent resonance.

KEYWORDS: Vertical axis wind turbine; orthogonal experiment method; finite element analysis; modal analysis.

INTRODUCTION

Wind is a ubiquitous resource. At present, wind energy is mainly used in wind power generation. In recent years, many countries have attached great importance to wind power generation, and wind power technology has developed rapidly. The use of wind turbines to generate electricity is the normal state in the field of power generation, and small vertical axis wind turbines have been widely used due to their small footprint and low cost.

Aykut Ozgun Onol et al.[1] presented a time-dependent, two-dimensional computational fluid dynamics (CFD) model coupled with the dynamics of the rotor for a height-normalized, small-scale high-solidity vertical axis wind turbine (VAWT) that consists of three straight blades, which are cambered to fit the circular path. Wu Zhenlong et al.[2] used the resolved gust approach (RGA) to simulate the gust transmission in the whole wind field, and studied the effect of lateral wind on the aerodynamic performance of vertical axis wind turbines. Lei Hang et al.[3] investigated the aerodynamic performance of a two-bladed vertical axis wind turbine using the turbulence model of the Improved Delayed Detached Eddy Simulation and the polyhedral mesh. Sahishnu R. Shah et al.[4] designed and modeled a small-scale vertical-axis wind turbine to meet low-demand application power supplies, and they studied the rotation performance of two new shapes of Savonius rotor blades against the conventional straight and curved blades. LI Qing'an et al.[5] evaluated the energy performance and aerodynamic force of a small vertical axis wind turbine with straight blades according to different tip velocity ratios through the wind tunnel test. Li Yan et al.[6] proposed a new method of connecting blades to rotor shaft for direct axis vertical axis wind turbine (SB-VAWT), which is called offset blade method. F. Arpino et al.[7] studied the performance of an innovative, real scale double-bladed wind turbine using a Reynolds Averaged Navier-Stokes-based CFD model.

Different from the above studies, this paper studies the influence of axial materials, blade materials and wind speed on the small vertical axis wind turbine and the natural frequency of wind wheel, and adopts the orthogonal experiment method (orthogonal experiment method is the experimental method of overall design, comprehensive comparison and statistical analysis of the experiment through orthogonal table),[8] in the case of different coaxial materials, blade materials and wind speed, ANSYS software is used to do the finite element analysis on the wind wheel part of the small vertical axis wind turbine, and the most reasonable design of the small vertical axis wind turbine is obtained; secondly, this paper uses ANSYS Workbench software,[9,10] to do modal analysis of the wind turbine,[11] and selects the model through data comparison.

1 Calculation settings

1.1 Material selection

In this paper, four kinds of blade materials including wood blade, fiber reinforced plastic blades, aluminum alloy extruded blade and carbon fiber composite blade and four kinds of

shaft materials including 45 steel, Q235-B carbon steel, 20Cr and 40Cr were selected for orthogonal experimental arrangement. The material properties of the four blades are shown in table 1. The material properties of the four axes are shown in table 2.

Table 1: The material properties of the four blades.

Material	Elastic modulus	Mass density	Poisson ratio
wood blade	12 GPa	1400 Kg/m^3	0.35
fiber reinforced plastic blade	24 GPa	2000 Kg/m^3	0.25
aluminum alloy extruded blade	70 GPa	2700 Kg/m^3	0.3
carbon fiber composite blade	120 GPa	1620 Kg/m^3	0.31

Table 2: The material properties of the four axes.

Material	Elastic modulus	Mass density	Poisson ratio
45 steel	209 GPa	7890 Kg/m^3	0.269
Q235-B carbon steel	210 GPa	7830 Kg/m^3	0.274
20Cr	207 GPa	7830 Kg/m^3	0.254
40Cr	211 GPa	7870 Kg/m^3	0.277

Choose to fix the geometry with a clamp on the underside of the wind wheel shaft. When the influence of other factors on the wind wheel is not considered, the same amount of pressure is applied to the five blades of the wind wheel.

1.2 Wind speed selection

This paper needs to consider different wind speeds, and select 12.5 m/s, 19 m/s, 26.5 m/s and 35 m/s for calculation and analysis.

1.3 Grid Computing

The wind wheel is gridded, and the grid size is selected according to the grid density to generate a grid with a good density. The total number of grids is 200,000, as shown in figure 1.

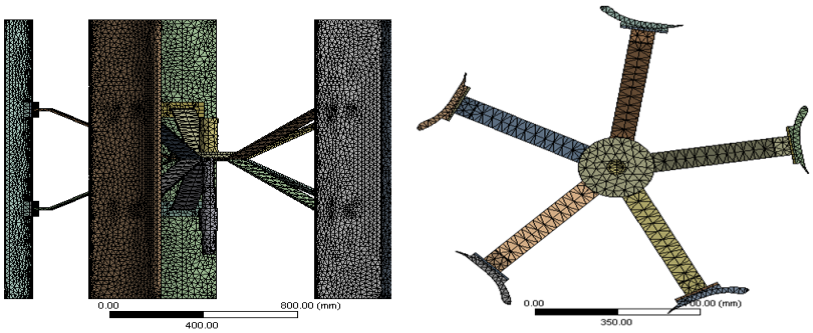

Figure 1: Meshing of wind wheel.

1.4 Design of orthogonal experiment table

This paper uses three factors and four levels of orthogonal experiment method, among which the three factors are wind blade material, shaft material and wind speed. The L16(4^3) orthogonal experiment table is established, as shown in table 3.

Table 3: The L 16(4^3) orthogonal experiment table.

Calculation scheme	Wind speed	Blade material	Shaft material
1	12.5 m/s	wood blade	40Cr
2	12.5 m/s	fiber reinforced plastic blade	20Cr
3	12.5 m/s	aluminum alloy extrusion blade	45 steel
4	12.5 m/s	carbon fiber composite blade	Q235-B carbon steel
5	19 m/s	wood blade	20Cr
6	19 m/s	fiber reinforced plastic blade	40Cr
7	19 m/s	aluminum alloy extrusion blade	Q235-B carbon steel
8	19 m/s	carbon fiber composite blade	45 steel
9	26.5 m/s	wood blade	45 steel
10	26.5 m/s	fiber reinforced plastic blade	Q235-B carbon steel
11	26.5 m/s	aluminum alloy extrusion blade	40Cr
12	26.5 m/s	carbon fiber composite blade	20Cr
13	35 m/s	wood blade	Q235-B carbon steel
14	35 m/s	fiber reinforced plastic blade	45 steel
15	35 m/s	aluminum alloy extrusion blade	20Cr
16	35 m/s	carbon fiber composite blade	40Cr

2 Finite element analysis

2.1 Results analysis

Calculation scheme 1: The wind speed load applied is 12.5 m/s, the blade material is wood blade, and the shaft material is 40Cr. Add a fluid with a density of 1.29 g/l, make the hydrostatic pressure on the blade be 12.5 m/s^2, and analyze it to obtain the combined displacement diagram and stress diagram of the wind wheel, as shown in figure 2.

Figure 2 (a) shows that the position of the maximum displacement is on the edge above the wind blade of the wind wheel, and the displacement is 0.022871 mm. The minimum displacement is on the bottom edge of the spindle, and the minimum displacement is 0 mm ; figure 2 (b) shows that the overall stress distribution of the wind wheel is uniform. The maximum stress on the wind wheel is on the bottom surface of the main shaft, and the stress is 0.71931 MPa, while the minimum stress on the wind wheel is 9.148e-12 MPa. The stress of wind blade changes little, and the whole is relatively uniform.

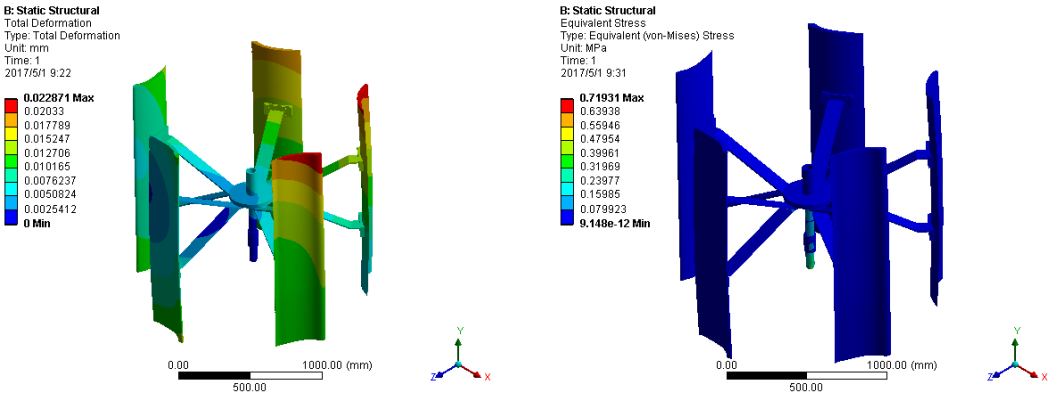

(a) Displacement diagram **(b) Stress diagram**

Figure 2: Combined displacement diagram and stress diagram of the wind wheel (wood-40Cr-12.5 m/s^2).

Calculation scheme 2: The wind speed load applied is 12.5 m/s, the blade material is fiber reinforced plastic blade, and the shaft material is 20Cr. Other conditions remain unchanged, the combined displacement diagram and stress diagram of the wind wheel are obtained, as shown in figure 3.

Figure 3 (a) shows that the position of the maximum displacement is on the edge above the wind blade of the wind wheel, and the displacement is 0.021629 mm. The minimum displacement is on the bottom edge of the spindle, and the minimum displacement is 0 mm ; figure 3 (b) shows that the overall stress distribution of the wind wheel is uniform. The maximum stress on the wind wheel is on the bottom surface of the main shaft, and the stress is 0.72413 MPa, while the minimum stress on the wind wheel is 6.5674e-12 MPa. The stress of wind blade changes little, and the whole is relatively uniform.

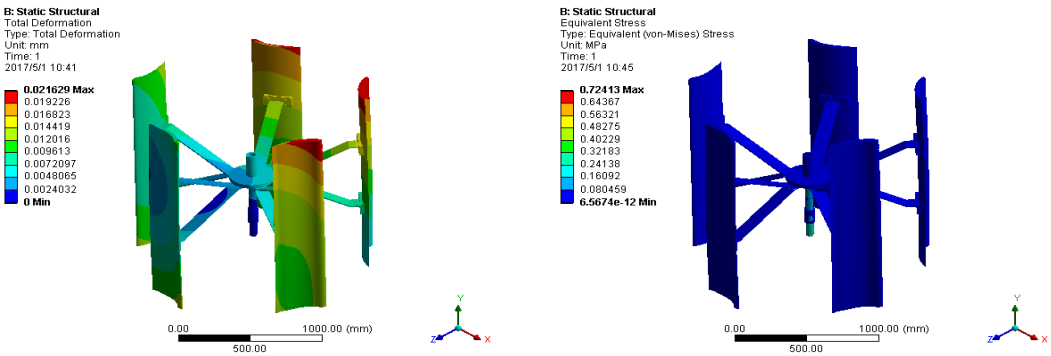

(a) Displacement diagram **(b) Stress diagram**

Figure 3: Combined displacement diagram and stress diagram of the wind wheel (fiber reinforced plastic-20Cr-12.5 m/s^2).

Calculation scheme 3: The wind speed load applied is 12.5 m/s, the blade material is aluminum alloy extrusion blade, and the shaft material is 45 steel. Other conditions remain unchanged, the combined displacement diagram and stress diagram of the wind wheel are obtained, as shown in figure 4.

Figure 4 (a) shows that the position of the maximum displacement is on the edge above the wind blade of the wind wheel, and the displacement is 0.021113 mm. The minimum displacement is on the bottom edge of the spindle, and the minimum displacement is 0 mm ; figure 4 (b) shows that the overall stress distribution of the wind wheel is uniform. The maximum stress on the wind wheel is on the bottom surface of the main shaft, and the stress is 0.72087 MPa, while the minimum stress on the wind wheel is 1.1015e-11 MPa. The stress of wind blade changes little, and the whole is relatively uniform.

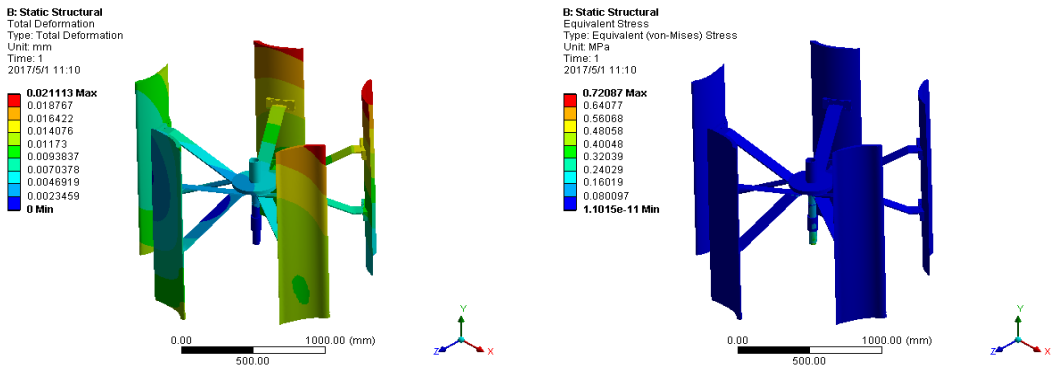

(a) Displacement diagram **(b) Stress diagram**

Figure 4: Combined displacement diagram and stress diagram of the wind wheel (aluminum alloy extrusion-45 steel-12.5 m/s^2).

Calculation scheme 4: The wind speed load applied is 12.5 m/s, the blade material is carbon fiber composite blade, and the shaft material is Q235-B carbon steel. Other conditions remain unchanged, the combined displacement diagram and stress diagram of the wind wheel are obtained, as shown in figure 5.

Figure 5 (a) shows that the position of the maximum displacement is on the edge above the wind blade of the wind wheel, and the displacement is 0.02099 mm. The minimum displacement is on the bottom edge of the spindle, and the minimum displacement is 0 mm ; figure 5 (b) shows that the overall stress distribution of the wind wheel is uniform. The maximum stress on the wind wheel is on the bottom surface of the main shaft, and the stress

is 0.71988 MPa, while the minimum stress on the wind wheel is 1.5311e-11 MPa. The stress of wind blade changes little, and the whole is relatively uniform.

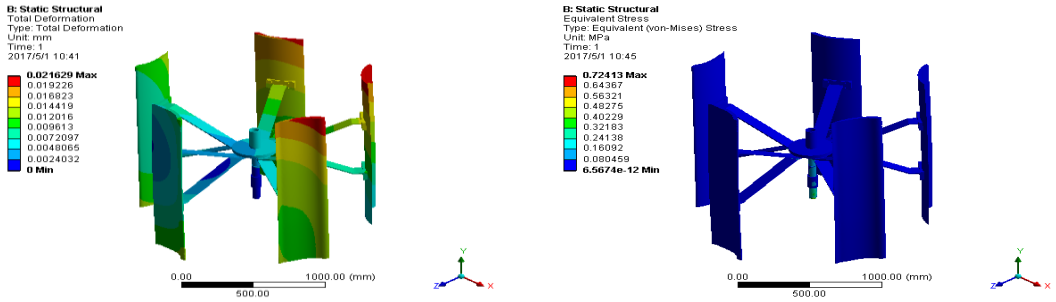

(a) Displacement diagram **(b) Stress diagram**

Figure 5: Combined displacement diagram and stress diagram of the wind wheel (carbon fiber composite-Q235-B carbon steel-12.5 m/s^2).

Calculation scheme 5: The wind speed load applied is 19 m/s, the blade material is wood blade, and the shaft material is 20Cr. Make the hydrostatic pressure on the blade be 19 m/s^2, the combined displacement diagram and stress diagram of the wind wheel are obtained, as shown in figure 6.

Figure 6 (a) shows that the position of the maximum displacement is on the edge above the wind blade of the wind wheel, and the displacement is 0.035171 mm. The minimum displacement is on the bottom edge of the spindle, and the minimum displacement is 0 mm ; figure 6 (b) shows that the overall stress distribution of the wind wheel is uniform. The maximum stress on the wind wheel is on the bottom surface of the main shaft, and the stress is 1.1006 MPa, while the minimum stress on the wind wheel is 1.4123e-11 MPa. The stress of wind blade changes little, and the whole is relatively uniform.

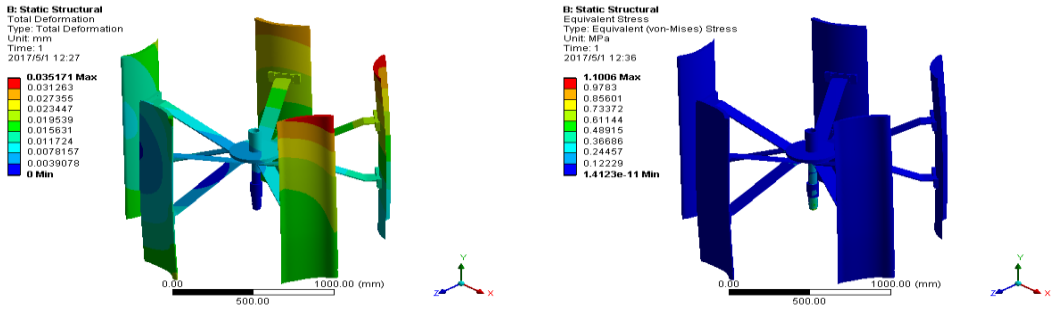

(a) Displacement diagram **(b) Stress diagram**

Figure 6: Combined displacement diagram and stress diagram of the wind wheel (wood-20Cr-19 m/s^2).

Calculation scheme 6: The wind speed load applied is 19 m/s, the blade material is fiber reinforced plastic blade, and the shaft material is 40Cr. Other conditions remain unchanged, the combined displacement diagram and stress diagram of the wind wheel are obtained, as shown in figure 7.

Figure 7 (a) shows that the position of the maximum displacement is on the edge above the wind blade of the wind wheel, and the displacement is 0.032471 mm. The minimum displacement is on the bottom edge of the spindle, and the minimum displacement is 0 mm ; figure 7 (b) shows that the overall stress distribution of the wind wheel is uniform. The maximum stress on the wind wheel is on the bottom surface of the main shaft, and the stress is 1.0934 MPa, while the minimum stress on the wind wheel is 9.8176e-12 MPa. The stress of wind blade changes little, and the whole is relatively uniform.

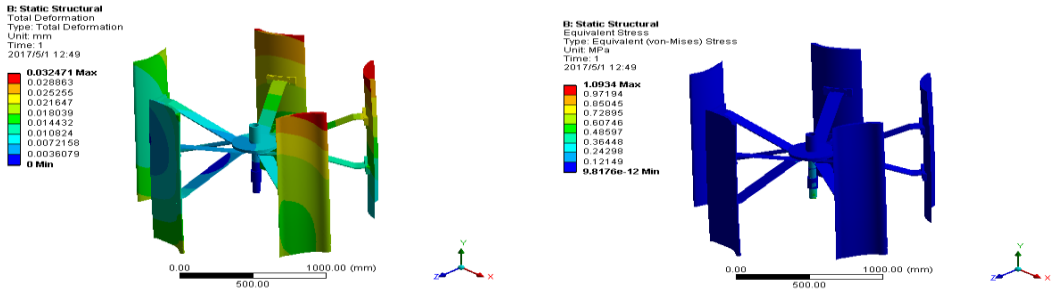

(a) Displacement diagram **(b) Stress diagram**

Figure 7: Combined displacement diagram and stress diagram of the wind wheel (fiber reinforced plastic-40Cr-19 m/s^2).

Calculation scheme 7: The wind speed load applied is 19 m/s, the blade material is aluminum alloy extrusion blade, and the shaft material is Q235-B carbon steel. Other conditions remain unchanged, the combined displacement diagram and stress diagram of the wind wheel are obtained, as shown in figure 8.

Figure 8 (a) shows that the position of the maximum displacement is on the edge above the wind blade of the wind wheel, and the displacement is 0.03199 mm. The minimum displacement is on the bottom edge of the spindle, and the minimum displacement is 0 mm ; figure 8 (b) shows that the overall stress distribution of the wind wheel is uniform. The maximum stress on the wind wheel is on the bottom surface of the main shaft, and the stress is 1.0942 MPa, while the minimum stress on the wind wheel is 1.6695e-11 MPa. The stress of wind blade changes little, and the whole is relatively uniform.

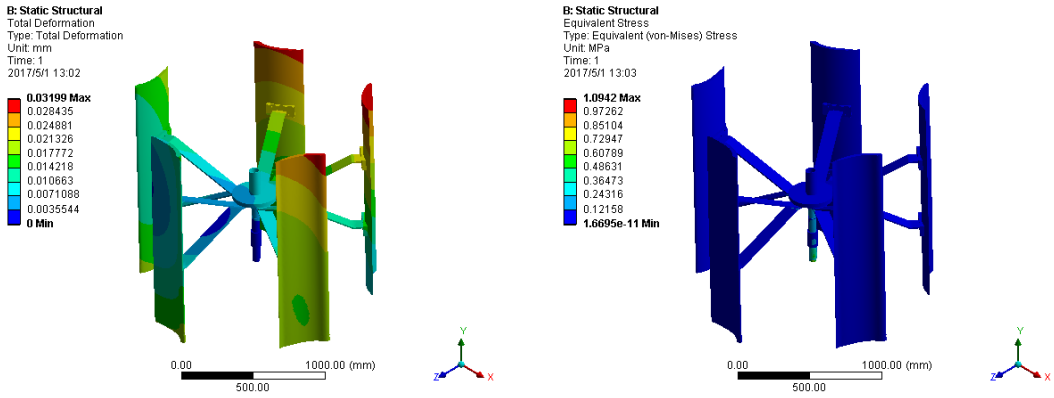

(a) Displacement diagram **(b) Stress diagram**

Figure 8: Combined displacement diagram and stress diagram of the wind wheel (aluminum alloy extrusion-Q235-B carbon steel-19 m/s^2).

Calculation scheme 8: The wind speed load applied is 19 m/s, the blade material is carbon fiber composite blade, and the shaft material is 45 steel. Other conditions remain unchanged, the combined displacement diagram and stress diagram of the wind wheel are obtained, as shown in figure 9.

Figure 9 (a) shows that the position of the maximum displacement is on the edge above the wind blade of the wind wheel, and the displacement is 0.032007 mm. The minimum displacement is on the bottom edge of the spindle, and the minimum displacement is 0 mm ; figure 9 (b) shows that the overall stress distribution of the wind wheel is uniform. The maximum stress on the wind wheel is on the bottom surface of the main shaft, and the stress is 1.0957 MPa, while the minimum stress on the wind wheel is 2.3681e-11 MPa. The stress of wind blade changes little, and the whole is relatively uniform.

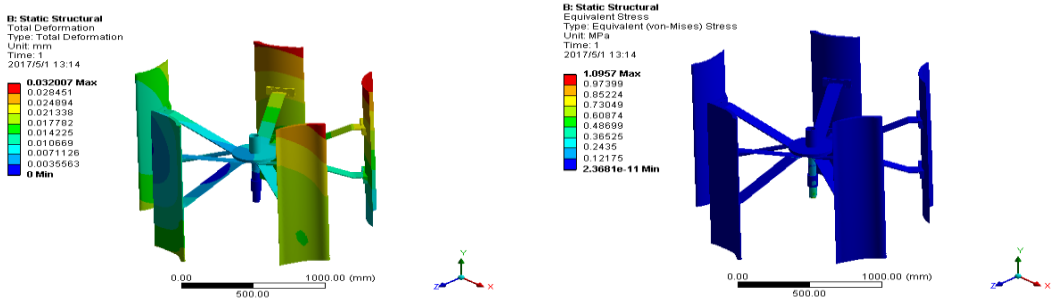

(a) Displacement diagram **(b) Stress diagram**

Figure 9: Combined displacement diagram and stress diagram of the wind wheel (carbon fiber composite-45 steel-19 m/s^2).

Calculation scheme 9: The wind speed load applied is 26.5 m/s, the blade material is wood blade, and the shaft material is 45 steel. Make the hydrostatic pressure on the blade be 26.5 m/s^2, the combined displacement diagram and stress diagram of the wind wheel are obtained, as shown in figure 10.

Figure 10 (a) shows that the position of the maximum displacement is on the edge above the wind blade of the wind wheel, and the displacement is 0.048784 mm. The minimum displacement is on the bottom edge of the spindle, and the minimum displacement is 0 mm ; figure 10 (b) shows that the overall stress distribution of the wind wheel is uniform. The maximum stress on the wind wheel is on the bottom surface of the main shaft, and the stress is 1.528 MPa, while the minimum stress on the wind wheel is 1.9529e-11 MPa. The stress of wind blade changes little, and the whole is relatively uniform.

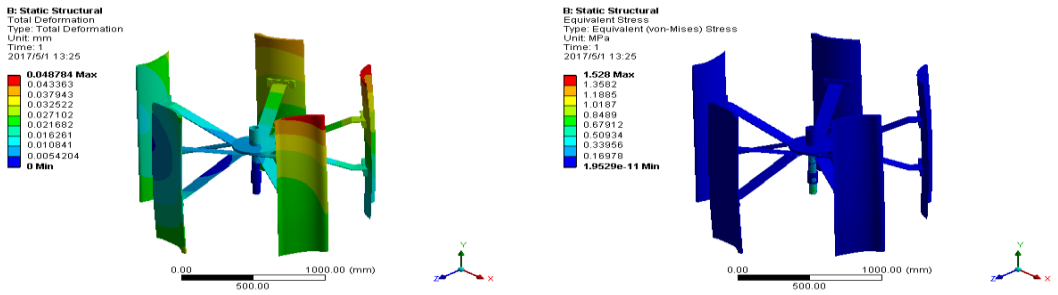

(a) Displacement diagram **(b) Stress diagram**

Figure 10: Combined displacement diagram and stress diagram of the wind wheel (wood-45 steel-26.5 m/s^2).

Calculation scheme 10: The wind speed load applied is 26.5 m/s, the blade material is fiber reinforced plastic blade, and the shaft material is Q235-B carbon steel. Other conditions remain unchanged, the combined displacement diagram and stress diagram of the wind wheel are obtained, as shown in figure 11.

Figure 11 (a) shows that the position of the maximum displacement is on the edge above the wind blade of the wind wheel, and the displacement is 0.04544 mm. The minimum displacement is on the bottom edge of the spindle, and the minimum displacement is 0 mm ; figure 11 (b) shows that the overall stress distribution of the wind wheel is uniform. The maximum stress on the wind wheel is on the bottom surface of the main shaft, and the stress is 1.526 MPa, while the minimum stress on the wind wheel is 1.3773e-11 MPa. The stress of wind blade changes little, and the whole is relatively uniform.

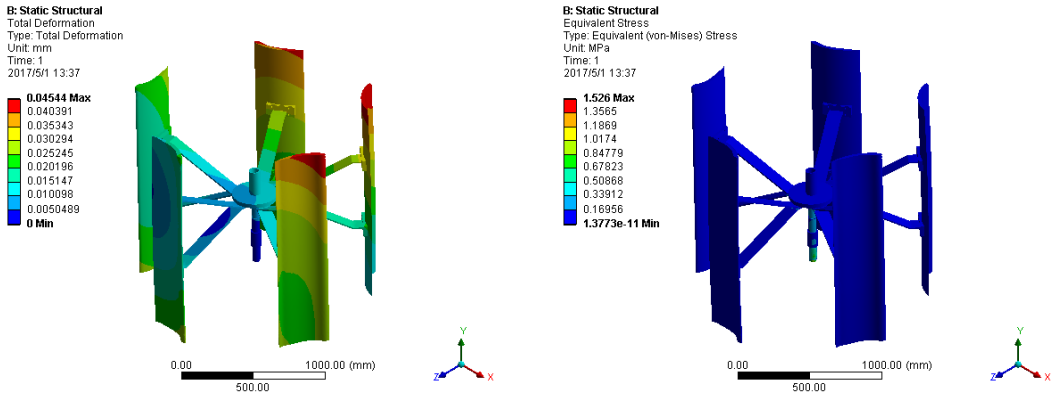

(a) Displacement diagram **(b) Stress diagram**

Figure 11: Combined displacement diagram and stress diagram of the wind wheel (fiber reinforced plastic-Q235-B carbon steel-26.5 m/s^2).

Calculation scheme 11: The wind speed load applied is 26.5 m/s, the blade material is aluminum alloy extrusion blade, and the shaft material is 40Cr. Other conditions remain unchanged, the combined displacement diagram and stress diagram of the wind wheel are obtained, as shown in figure 12.

Figure 12 (a) shows that the position of the maximum displacement is on the edge above the wind blade of the wind wheel, and the displacement is 0.044458 mm. The minimum displacement is on the bottom edge of the spindle, and the minimum displacement is 0 mm ; figure 12 (b) shows that the overall stress distribution of the wind wheel is uniform. The maximum stress on the wind wheel is on the bottom surface of the main shaft, and the stress is 1.5251 MPa, while the minimum stress on the wind wheel is 2.3472e-11 MPa. The stress of wind blade changes little, and the whole is relatively uniform.

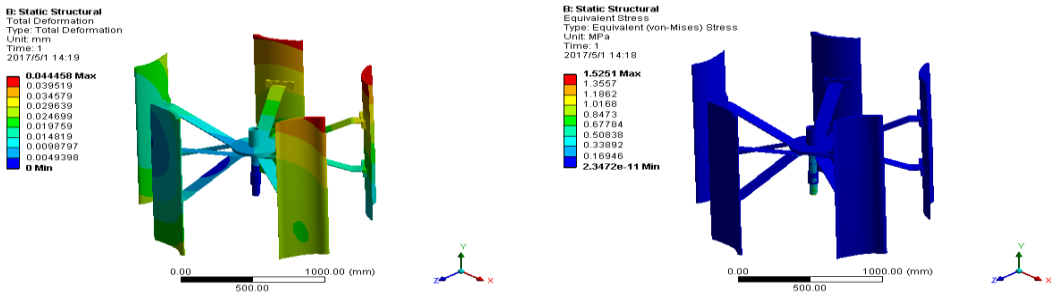

(a) Displacement diagram **(b) Stress diagram**

Figure 12: Combined displacement diagram and stress diagram of the wind wheel (aluminum alloy extrusion-40Cr-26.5 m/s^2).

Calculation scheme 12: The wind speed load applied is 26.5 m/s, the blade material is carbon fiber composite blade, and the shaft material is 20Cr. Other conditions remain unchanged, the combined displacement diagram and stress diagram of the wind wheel are obtained, as shown in figure 13.

Figure 13 (a) shows that the position of the maximum displacement is on the edge above the wind blade of the wind wheel, and the displacement is 0.044885 mm. The minimum displacement is on the bottom edge of the spindle, and the minimum displacement is 0 mm ; figure 13 (b) shows that the overall stress distribution of the wind wheel is uniform. The maximum stress on the wind wheel is on the bottom surface of the main shaft, and the stress is 1.5353 MPa, while the minimum stress on the wind wheel is 3.2688e-11 MPa. The stress of wind blade changes little, and the whole is relatively uniform.

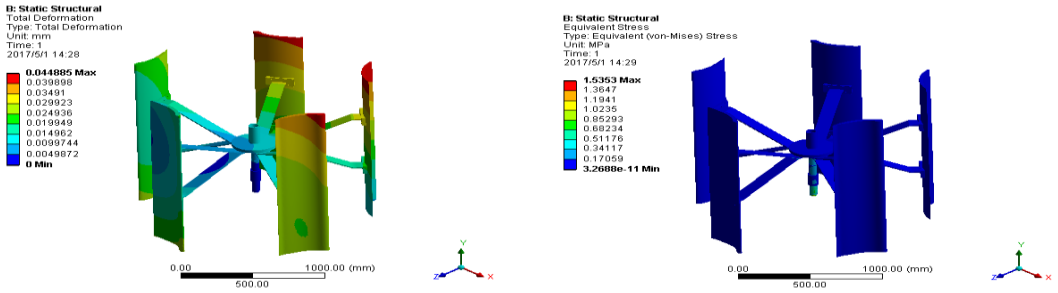

(a) Displacement diagram **(b) Stress diagram**

Figure 13: Combined displacement diagram and stress diagram of the wind wheel (carbon fiber composite-20Cr-26.5 m/s^2).

Calculation scheme 13: The wind speed load applied is 35 m/s, the blade material is wood blade, and the shaft material is Q235-B carbon steel. Make the hydrostatic pressure on the blade be 35 m/s^2, the combined displacement diagram and stress diagram of the wind wheel are obtained, as shown in figure 14.

Figure 14 (a) shows that the position of the maximum displacement is on the edge above the wind blade of the wind wheel, and the displacement is 0.064239 mm. The minimum displacement is on the bottom edge of the spindle, and the minimum displacement is 0 mm ; figure 14 (b) shows that the overall stress distribution of the wind wheel is uniform. The maximum stress on the wind wheel is on the bottom surface of the main shaft, and the stress is 2.0153 MPa, while the minimum stress on the wind wheel is 2.5701e-11 MPa. The stress of wind blade changes little, and the whole is relatively uniform.

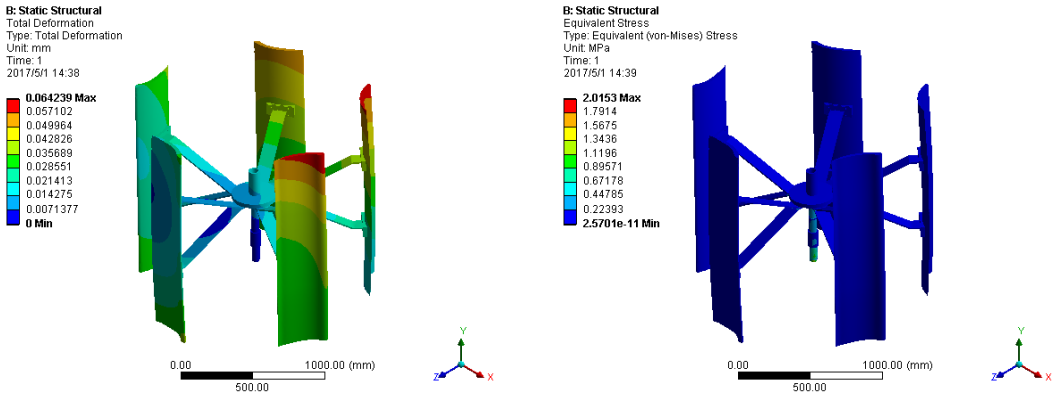

(a) Displacement diagram **(b) Stress diagram**

Figure 14: Combined displacement diagram and stress diagram of the wind wheel (wood-Q235-B carbon steel-35 m/s^2).

Calculation scheme 14: The wind speed load applied is 35 m/s, the blade material is fiber reinforced plastic blade, and the shaft material is 45 steel. Other conditions remain unchanged, the combined displacement diagram and stress diagram of the wind wheel are obtained, as shown in figure 15.

Figure 15 (a) shows that the position of the maximum displacement is on the edge above the wind blade of the wind wheel, and the displacement is 0.060207 mm. The minimum displacement is on the bottom edge of the spindle, and the minimum displacement is 0 mm ; figure 15 (b) shows that the overall stress distribution of the wind wheel is uniform. The maximum stress on the wind wheel is on the bottom surface of the main shaft, and the stress is 2.0183 MPa, while the minimum stress on the wind wheel is 1.8242e-11 MPa. The stress of wind blade changes little, and the whole is relatively uniform.

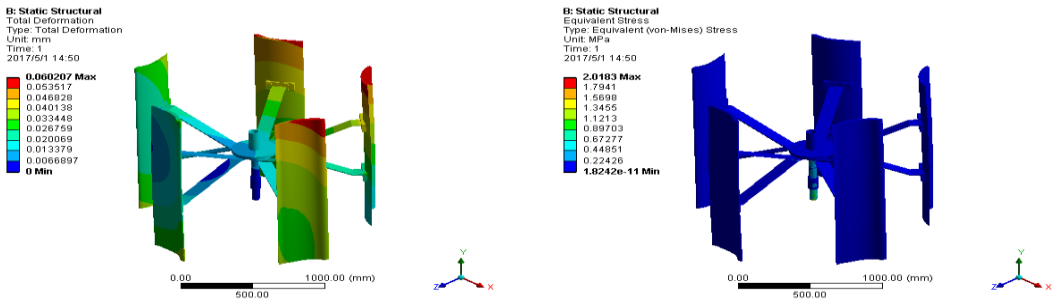

(a) Displacement diagram **(b) Stress diagram**

Figure 15: Combined displacement diagram and stress diagram of the wind wheel (fiber reinforced plastic-45 steel-35 m/s^2).

Calculation scheme 15: The wind speed load applied is 35 m/s, the blade material is aluminum alloy extrusion blade, and the shaft material is 20Cr. Other conditions remain unchanged, the combined displacement diagram and stress diagram of the wind wheel are obtained, as shown in figure 16.

Figure 16 (a) shows that the position of the maximum displacement is on the edge above the wind blade of the wind wheel, and the displacement is 0.059439 mm. The minimum displacement is on the bottom edge of the spindle, and the minimum displacement is 0 mm ; figure 16 (b) shows that the overall stress distribution of the wind wheel is uniform. The maximum stress on the wind wheel is on the bottom surface of the main shaft, and the stress is 2.0277 MPa, while the minimum stress on the wind wheel is 3.1646e-11 MPa. The stress of wind blade changes little, and the whole is relatively uniform.

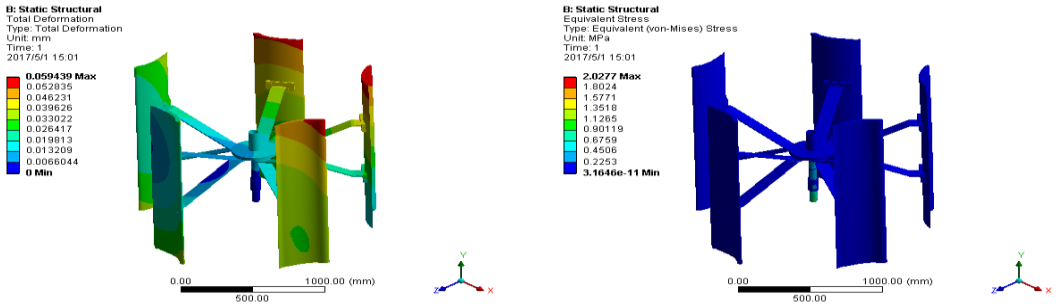

(a) Displacement diagram **(b) Stress diagram**

Figure 16: Combined displacement diagram and stress diagram of the wind wheel (aluminum alloy extrusion-20Cr-35 m/s^2).

Calculation scheme 16: The wind speed load applied is 35 m/s, the blade material is carbon fiber composite blade, and the shaft material is 40Cr. Other conditions remain unchanged, the combined displacement diagram and stress diagram of the wind wheel are obtained, as shown in figure 17.

Figure 17 (a) shows that the position of the maximum displacement is on the edge above the wind blade of the wind wheel, and the displacement is 0.058561 mm. The minimum displacement is on the bottom edge of the spindle, and the minimum displacement is 0 mm ; figure 17 (b) shows that the overall stress distribution of the wind wheel is uniform. The maximum stress on the wind wheel is on the bottom surface of the main shaft, and the stress is 2.0144 MPa, while the minimum stress on the wind wheel is 4.3894e-11 MPa. The stress of wind blade changes little, and the whole is relatively uniform.

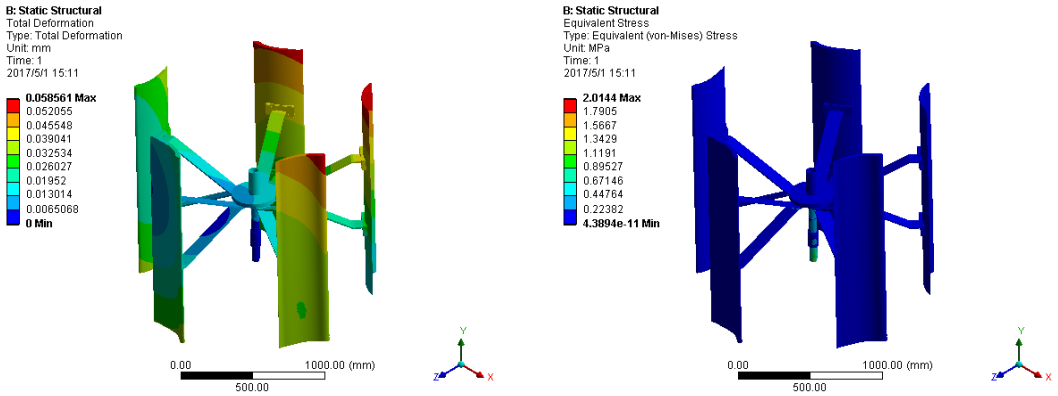

(a) Displacement diagram **(b) Stress diagram**

Figure 17: Combined displacement diagram and stress diagram of the wind wheel (carbon fiber composite-40Cr-35 m/s^2).

2.2 Maximum displacement and stress

According to the experimental data, draw the relationship between the experimental number and the maximum displacement, as shown in figure 18. The relationship between the experimental number and the maximum stress is shown in figure 19.

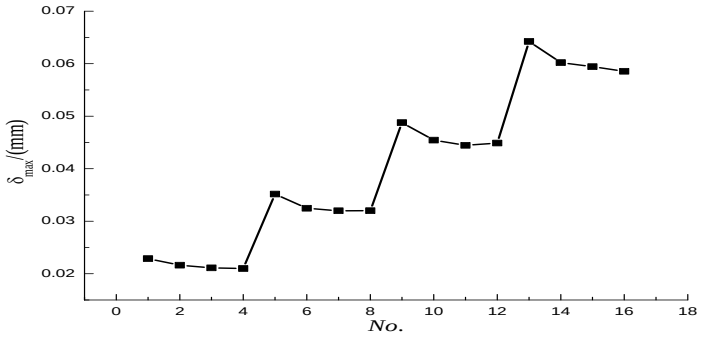

Figure 18: The relationship between the experimental number and the maximum displacement.

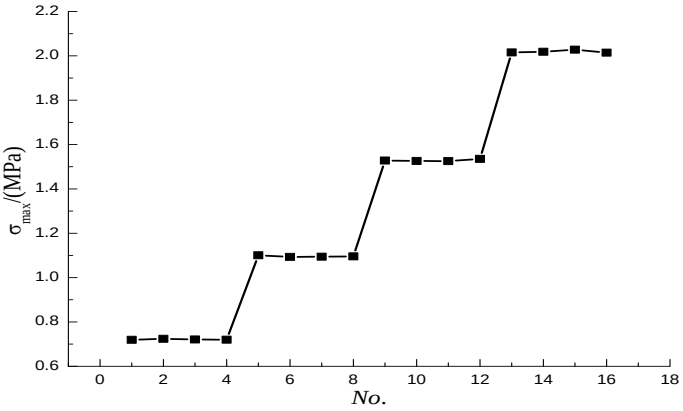

Figure 19: The relationship between the experimental number and the maximum stress.

Figures 18 and 19 show that the wind speed does not change, the maximum displacement decreases in turn, and the maximum stress remains almost unchanged. Each time the wind speed increases, the maximum displacement and maximum stress will increase significantly. When the wind speed is small, the displacement and stress of shaft material and blade material change little. Based on the change of wind speed of 35 m/s, comparing the maximum displacement and maximum stress, it is found that when the shaft material is 40Cr and the blade material is carbon fiber composite material, the wind wheel system is the most stable.

3 Modal Analysis

3.1 Wind wheel modals

In the modal analysis of vertical axis wind turbine, the wind wheel structure is mainly subjected to periodic excitation. The modal distribution of wind wheel is obtained by ANSYS Workbench analysis, as shown in figure 20.

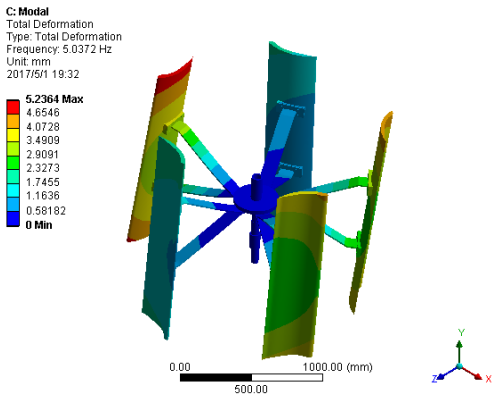

(a) First-order modal

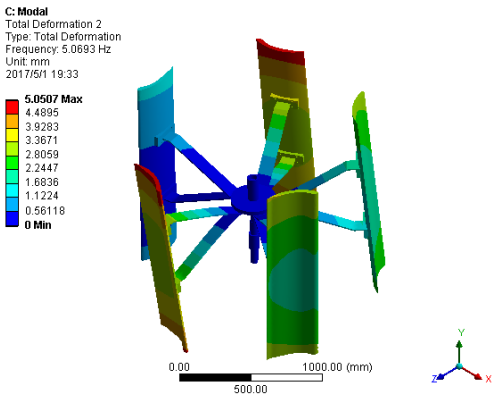

(b) Second-order mode

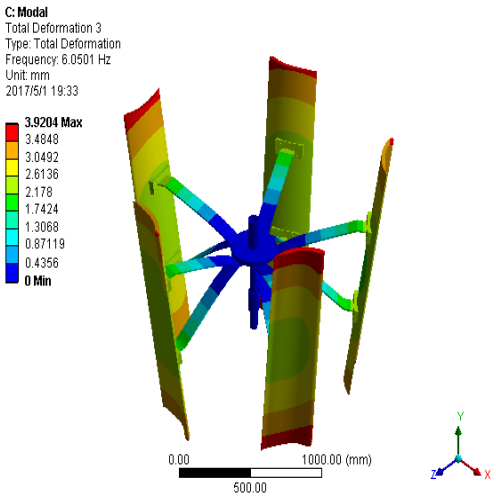

(c) Third-order mode

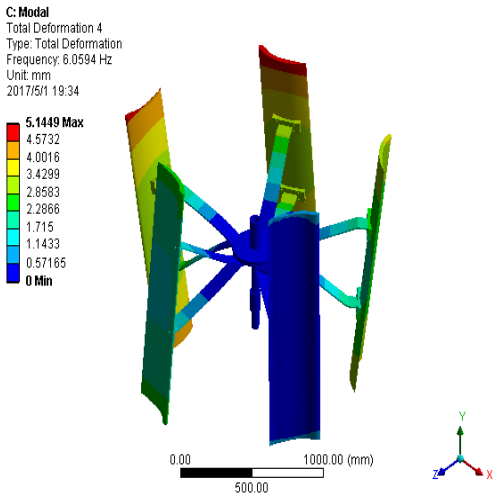

(d) Fourth-order mode

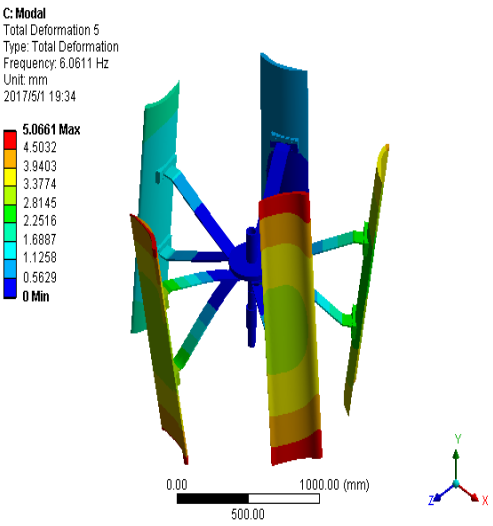

(e) Fifth-order mode

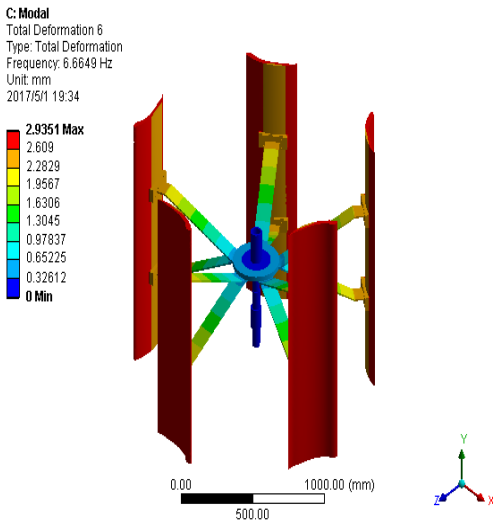

(f) Sixth-order mode

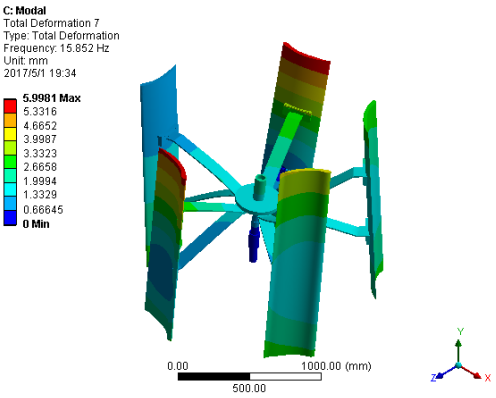

(g) Seventh-order mode

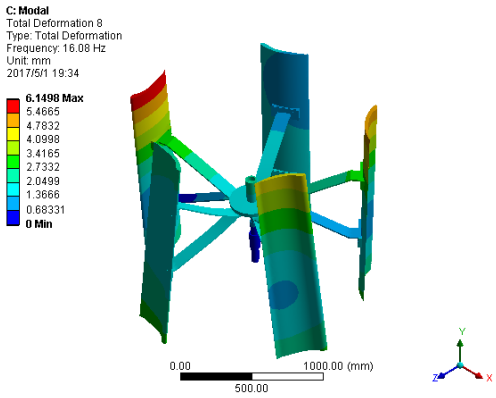

(h) Eighth-order mode

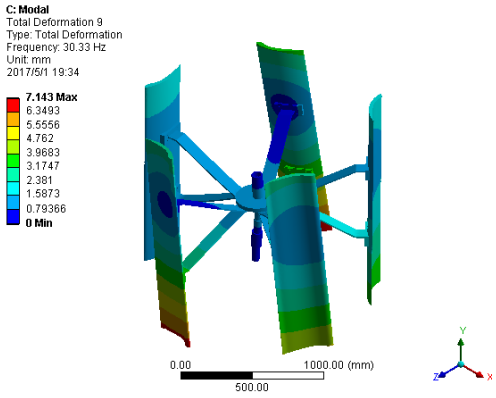

(i) Ninth-order mode

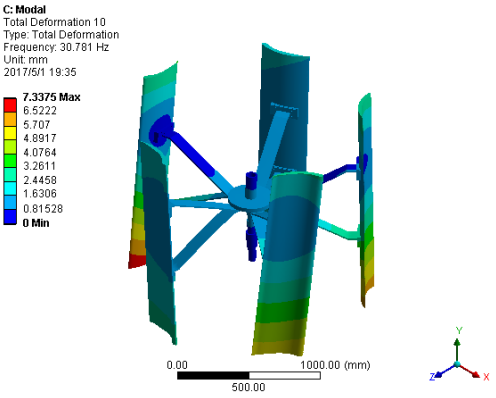

(j) Tenth-order mode

Figure 20: Distribution of wind wheel modes.

3.2 Natural frequency

Modal analysis is conducted by ANSYS Workbench software to obtain the wind wheel structure frequency, as shown in figure 21.

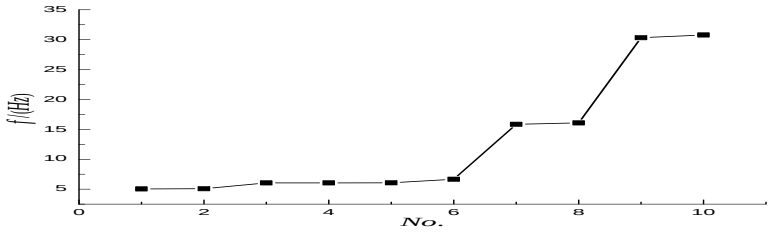

Figure 21: Frequency of wind wheel structure.

It can be seen from figure 21 that the frequency of the structure of the wind wheel is generally increasing. When the first-order mode changes to the sixth-order mode, the seventh-order mode changes to the eighth-order mode, and the ninth-order mode changes to the ten-order mode, the frequency increase of wind wheel structure is small. When the sixth-order mode changes to the seventh-order mode and the eighth-order mode changes to the ninth-order mode, the frequency of wind turbine structure increases greatly. The third-order mode has a higher chance of appearing in practice, so it is used as the natural frequency of the wind turbine structure. The frequency added by the wind wheel should avoid 6.05 *Hz* to prevent resonance.

4. CONCLUSION

This paper uses ANSYS software to carry out the three-dimensional modeling of small vertical axis wind turbines; uses orthogonal experiments to establish orthogonal experiment tables; uses ANSYS Workbench software to make a finite element analysis of the wind wheel part of a small vertical axis wind turbine by changing the shaft material, blade material and wind speed. It is found that the maximum displacement always occurs in the upper part of the blade of the wind wheel, and the maximum stress is always in the bottom surface of the main shaft of the wind wheel. When the wind speed is constant, the maximum displacement tends to decrease and the maximum stress remains almost unchanged. And each time the wind speed increases, the maximum displacement and maximum stress will increase significantly. When the wind speed is small, the displacement and stress of axial material and blade material change little. After comparative analysis, it is determined that the best choice is when the axial material is 40Cr and the blade material is carbon fiber composite blade; After modal analysis using ANSYS Workbench software, it is found that the frequency of wind

wheel structure changes little from the first-order mode to the sixth-order mode. The third-order mode has a higher chance of appearing in practice, so it is used as the natural frequency of the wind turbine structure. The frequency added by the wind wheel should avoid 6.05 *Hz* to prevent resonance.

REFERENCES

1. Aykut Ozgun Onol, Serhat Yesilyurt. Effects of wind gusts on a vertical axis wind turbine with high solidity [J]. Journal of Wind Engineering Industrial Aerodynamics, 2017; 162: 1-11.
2. Wu Zhenlong, Galih Bangga, Cao Yihua. Effects of lateral wind gusts on vertical axis wind turbines [J]. Energy, 2019; 167(C): 1212-1223.
3. Lei Hang, Zhou Dai, Bao Yan. Three-dimensional improved delayed detached eddy simulation of a two-bladed vertical axis wind turbine [J]. Energy Conversion and Management, 2017; 133: 235-248.
4. Sahishnu R. Shah, Rakesh Kumar, Kaamran Raahemifar. Design, modeling and economic performance of a vertical axis wind turbine [J]. Energy Reports, 2018; 4: 619-623.
5. Li Qing'an, Takao Maeda, Yasunari Kamada. Analysis of aerodynamic Load on straight-bladed vertical axis wind turbine [J]. Journal of Thermal Science, 2014; 23(04): 315-324.
6. Li Yan, Zhao Shouyang, Qu Chunming. Effects of Offset Blade on Aerodynamic Characteristics of Small-Scale Vertical Axis Wind Turbine [J]. Journal of Thermal Science, 2019; 28(02): 326-339.
7. F. Arpino, M. Scungio, G. Cortellessa. Numerical performance assessment of an innovative Darrieus-style vertical axis wind turbine with auxiliary straight blades [J]. Energy Conversion and Management, 2018; 171: 769-777.
8. Cai Shibo, Bao Guanjun, Ma Xiaolong. Parameters optimization of the dust absorbing structure for photovoltaic panel cleaning robot based on orthogonal experiment method [J]. Journal of Cleaner Production, 2019; 217: 724-731.
9. Li Zhaocan, Xu Kun. Optimal design of rotary tool based on ANSYS Workbench [J]. International Journal of Plant Engineering and Management, 2017; 22(01): 59-64.
10. Jing Pingan, Wang Zhongmin. Study on finite element analysis of a folding crane based on ANSYS Workbench [J]. International Journal of Plant Engineering and Management, 2015; 20(04): 233-239.
11. Jia Jianwei. Modal analysis of hydraulic winch transmission shaft based on ANSYS Workbench [J]. Coal mine machinery, 2019; 40(07): 82-83.